International Journal of
Molecular Sciences

MDPI

Article

DNA Methylation Alterations in Fractionally Irradiated Rats and Breast Cancer Patients Receiving Radiotherapy

Magy Sallam [1,2], Mohamed Mysara [1,†], Mohammed Abderrafi Benotmane [1], Radia Tamarat [3], Susana Constantino Rosa Santos [4], Anne P. G. Crijns [5], Daan Spoor [5], Filip Van Nieuwerburgh [6], Dieter Deforce [6], Sarah Baatout [1,7], Pieter-Jan Guns [2], An Aerts [1,‡] and Raghda Ramadan [1,*,‡]

1 Radiobiology Unit, Interdisciplinary Biosciences, Belgian Nuclear Research Centre, SCK CEN, 2400 Mol, Belgium
2 Laboratory of Physiopharmacology, University of Antwerp, 2610 Wilrijk, Belgium
3 Institut de Radioprotection et de Sureté Nucléaire (IRSN), PRP-HOM, SRBE, LR2I, 92260 Fontenay-aux-Roses, France
4 Centro Cardiovascular da Universidade de Lisboa (CCUL@RISE), Lisbon School of Medicine of the Universidade de Lisboa, 1649-028 Lisbon, Portugal
5 Department of Radiation Oncology, University Medical Center Groningen, University of Groningen, 9713 GZ Groningen, The Netherlands
6 Laboratory of Pharmaceutical Biotechnology, Ghent University, 9000 Ghent, Belgium
7 Department of Molecular Biotechnology, Ghent University, 9000 Ghent, Belgium
* Correspondence: raghda.ramadan@sckcen.be
† Current affiliation: Bioinformatics Group, Center for Informatics Sciences (CIS), School of Information Technology and Computer Science (ICTS), Nile University, Giza 12588, Egypt.
‡ These authors share last authorship.

Citation: Sallam, M.; Mysara, M.; Benotmane, M.A.; Tamarat, R.; Santos, S.C.R.; Crijns, A.P.G.; Spoor, D.; Van Nieuwerburgh, F.; Deforce, D.; Baatout, S.; Guns, P.-J.; Aerts, A.; et al. DNA Methylation Alterations in Fractionally Irradiated Rats and Breast Cancer Patients Receiving Radiotherapy. *Int. J. Mol. Sci.* **2022**, *23*, 16214. https://doi.org/10.3390/ijms232416214

Academic Editor: Andreyan N. Osipov

Received: 21 November 2022
Accepted: 15 December 2022
Published: 19 December 2022
Corrected: 18 December 2023

Abstract: Radiation-Induced CardioVascular Disease (RICVD) is an important concern in thoracic radiotherapy with complex underlying pathophysiology. Recently, we proposed DNA methylation as a possible mechanism contributing to RICVD. The current study investigates DNA methylation in heart-irradiated rats and radiotherapy-treated breast cancer (BC) patients. Rats received fractionated whole heart X-irradiation (0, 0.92, 6.9 and 27.6 Gy total doses) and blood was collected after 1.5, 3, 7 and 12 months. Global and gene-specific methylation of the samples were evaluated; and gene expression of selected differentially methylated regions (DMRs) was validated in rat and BC patient blood. In rats receiving an absorbed dose of 27.6 Gy, DNA methylation alterations were detected up to 7 months with differential expression of cardiac-relevant DMRs. Of those, *SLMAP* showed increased expression at 1.5 months, which correlated with hypomethylation. Furthermore, *E2F6* inversely correlated with a decreased global longitudinal strain. In BC patients, *E2F6* and *SLMAP* exhibited differential expression directly and 6 months after radiotherapy, respectively. This study describes a systemic radiation fingerprint at the DNA methylation level, elucidating a possible association of DNA methylation to RICVD pathophysiology, to be validated in future mechanistic studies.

Keywords: DNA methylation; gene expression; cardiovascular disease; ionizing radiation; breast cancer patient

1. Introduction

Thoracic radiotherapy has been shown to increase the risk of cardiac toxicity in cancer patients [1–3]. Despite the current radiation-sparing techniques, which limit cardiac exposure, radiation-induced cardiovascular disease (RICVD) is still a primary clinical concern that manifests mainly as coronary heart disease, remaining asymptomatic until 10 to 15 years after radiotherapy [4]. However, a 6% decrease in global longitudinal strain (GLS), an early sign of subclinical left ventricular dysfunction, has been reported in breast cancer (BC) patients as early as 6 months after radiotherapy [5,6]. Consequently, investigating early molecular changes in the cardiovascular system after radiotherapy could

identify novel, unexamined players in RICVD pathology and/or potential biomarkers to identify patients at risk, thereby allowing earlier countermeasures.

DNA methylation is an epigenetic process essential for development and maintenance of cellular homeostasis, normally associated with transcriptional silencing when affecting gene promoters [7,8]. Alterations in DNA methylation have been reported in many diseases, including neurodegenerative diseases such as Parkinson's disease [9], diabetes mellitus [10] and cancer [11]. In addition, recent research indicates a connection between DNA methylation and cardiovascular disease risk [12,13] with methylation alterations preceding histologically evident atherosclerosis [14]. DNA methylation has been hypothesized to affect atherosclerosis pathogenesis by regulating oxidative stress, inflammation and vascular smooth muscle cell (VSMC) phenotype [15]. Interestingly, radiation has also been shown to affect DNA methylation. Both radiation-induced global hypomethylation, as well as gene-specific hypermethylation, have been reported [4,16,17]. However, the contribution of DNA methylation in X-irradiation-induced cardiac toxicity is underexplored. Consequently, the current study aims to investigate the effects of ionizing radiation on DNA methylation in the blood of irradiated rats and BC patients to provide more clarity on the involvement of DNA methylation in RICVD.

The current study is part of the Horizon 2020 project MEDIRAD (http://www.medirad-project.eu, accessed on 30 June 2021) which addresses the implications of medical low-dose radiation exposure [18]. Within MEDIRAD, the effect of radiation on cardiac dysfunction is investigated using preclinical and clinical experimental models [19,20]. In the current study, we assess the methylation profile of irradiated rats of the preclinical model, with special focus on cardiac-relevant differentially methylated regions (DMRs). We also investigate the expression profile of the cardiac-relevant rat-identified DMRs in 25 BC patients from the MEDIRAD EARLY-HEART cohort, the latter cohort being a European multicenter study involving 250 BC patients treated with adjuvant radiotherapy and followed up for 2 years after initial treatment [20].

2. Results

2.1. Global Hypomethylation Observed at 12 Months after Whole Heart Rat Irradiation

The percentage of 5-methyl cytosine (5 mC%) in rat blood DNA after the different irradiation doses at the four sampling time points is shown in Figure 1. The irradiated rats exhibited dose-dependent reduction in global longitudinal strain (GLS) (>15%), as measured by echocardiography, at 12 and 18 months, along with decreased cardiac apex microvascular density after 27.6 Gy [19]. Significant hypomethylation was observed at 12 months after all irradiation doses relative to sham-irradiated rats. This is especially evident in rats irradiated with 0.92 and 6.9 Gy with significantly lower methylation levels observed at 7 and 12 months relative to 1.5 months. Global hypomethylation, as measured by 5 mC%, strongly correlated with the GLS of rats receiving 6.9 and 27.6 Gy at 12 months after fractionated irradiation (FI) ($r = |0.998|$, p-value < 0.05 and $r = |0.884|$, p-value $= 0.12$, respectively; Supplementary Figure S1).

2.2. Gene-Specific DNA Methylation Analysis and Enriched Pathways of Rat DMRs

A total of 67,098 and 684,433 DMRs were identified across all chromosomes at 1.5 and 7 months after 27.6 Gy FI relative to sham-irradiated rats, respectively. After DMR filtering according to significance (p-value < 0.05), the number of DMRs dropped to 7344 and 8620 at 1.5 and 7 months, respectively (a detailed list of DMRs is provided in Supplementary Materials). Of those, 3933 and 4710 DMRs were hypomethylated while 3411 and 3910 DMRs were hypermethylated at 1.5 and 7 months after irradiation, respectively (Figure 2).

Pathway analysis of significant DMRs (p-value < 0.05) revealed the enrichment of several pathways, including the dilated cardiomyopathy pathway at both 1.5 and 7 months (Figure 3). Other cardiac relevant KEGG pathways were also enriched at 1.5 months (adrenergic signaling in cardiomyocytes, cardiac muscle contraction, hypertrophic cardiomyopathy, arrhythmogenic right ventricular cardiomyopathy, calcium signaling pathway and

Hippo signaling pathway) as well as at 7 months (regulation of actin cytoskeleton and tight junction).

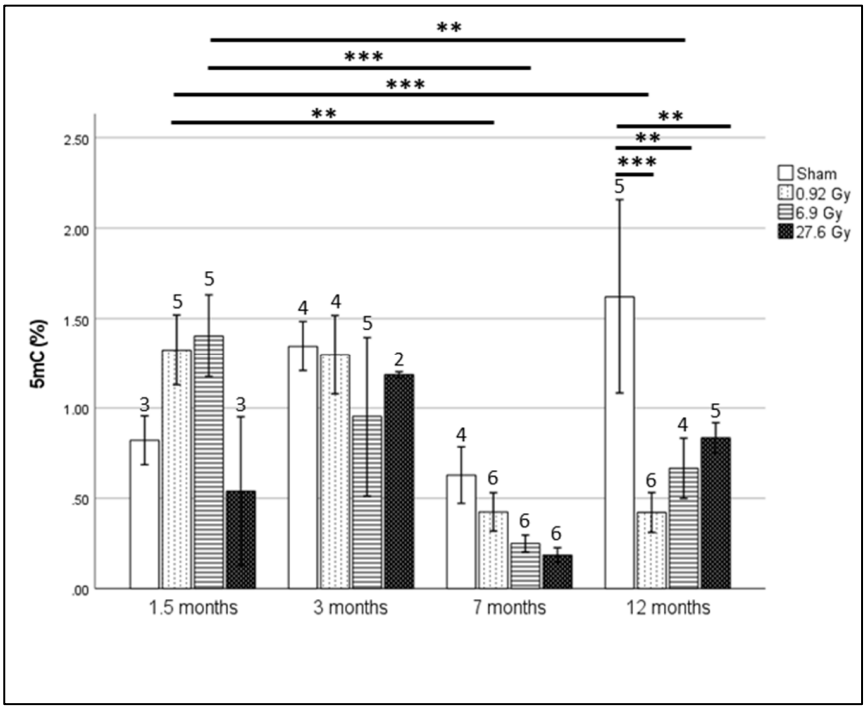

Figure 1. Percentage of 5 mC (%) after fractionated irradiation of 0, 0.04, 0.3 and 1.2 Gy resulting in total irradiation dose of 0, 0.92, 6.9 and 27.6 Gy as measured by MethylFlash Global DNA Methylation (5 mC) ELISA Easy Kit at 1.5, 3, 7 and 12 months after irradiation. Plotted values represent group means ± standard error of mean (SEM) with the number of rats per group indicated per bar. Statistical analysis was performed using SPSS generalized linear model module and multiple comparison correction was performed using least significant difference (LSD) (** = *p*-value < 0.01, *** < 0.001).

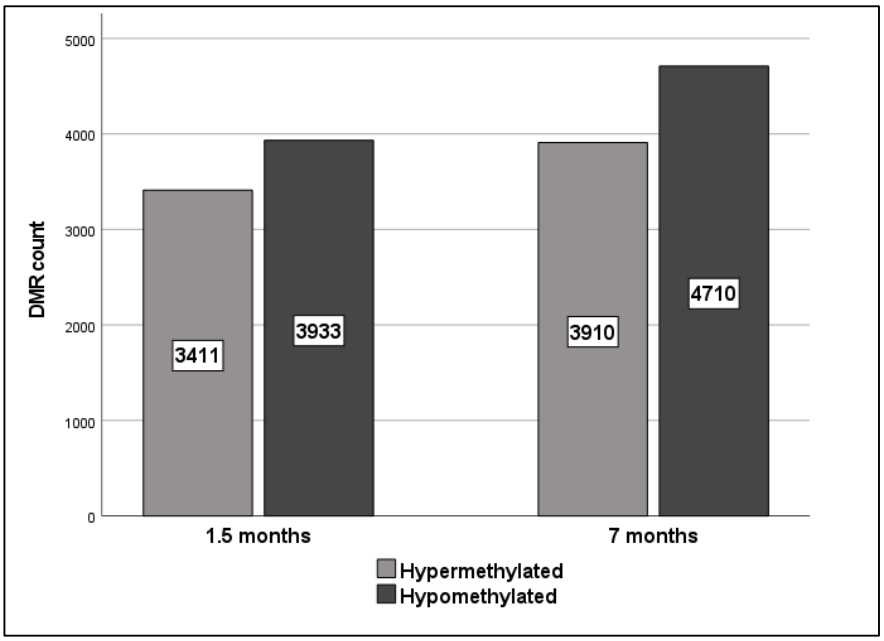

Figure 2. Significant hyper- (pale grey) and hypo- (dark grey) methylated DMR counts (*p*-value < 0.05) identified by SureSelect MethylSeq in rats receiving 27.6 Gy FI relative to sham-irradiated rats at 1.5 and 7 months after irradiation.

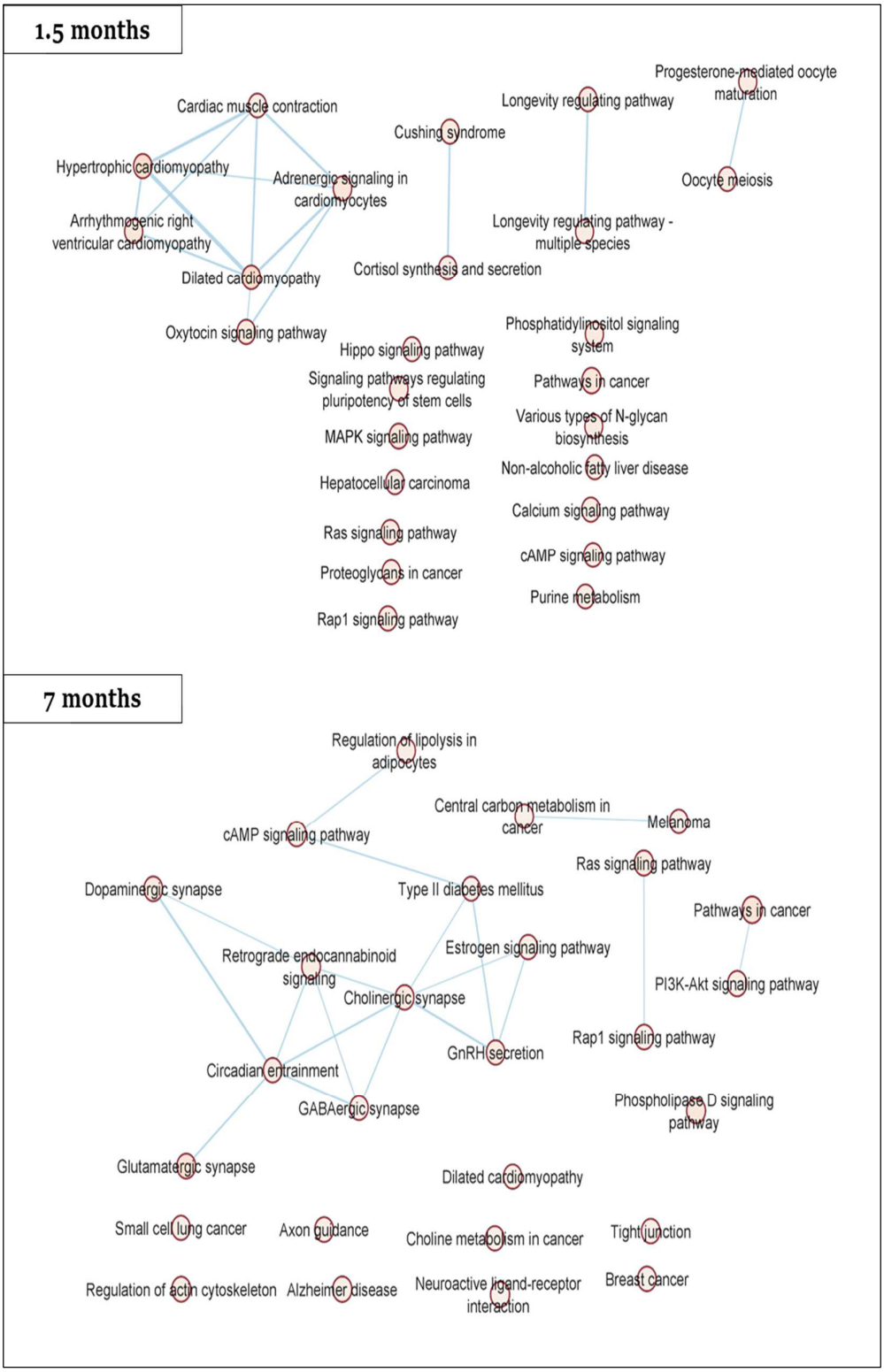

Figure 3. Pathway analysis of significant DMRs (p-value < 0.05). Statistically significant KEGG pathways (p-value < 0.05, Q-value < 0.25) were visualized by STRING-db and Cytoscape, respectively.

For downstream qPCR validation, cutoff criteria were applied yielding 10 and 24 DMRs at 1.5 and 7 months, respectively (detailed in Supplementary Materials). Next, the DMR list was further reduced by selection of DMRs previously linked to cardiovascular function in literature. A qPCR validation was performed for 8 DMRs (*SLMAP*, *LDLR*, *ITPR2*, *CDH18*, *CACNA1C*, *CELF4*, *E2F6* and *PTPN2)*. A brief description of these genes, as well as

their connection to cardiovascular function/disease and observed methylation status, is provided in Table 1.

Table 1. DMRs selected for downstream validation, their correlation to cardiovascular function/disease and their altered methylation status after 27.6 Gy FI.

DMR	Connection to Cardiac Function/Disease	Methylation State after 27.6 Gy FI Dose Relative to Sham Irradiated Rats (p-Value < 0.05)
SLMAP (*Sarcolemma Associated Protein*)	*SLMAP* is a component of cardiac membranes involved in excitation-contraction (E-C) coupling and its perturbation results in progressive deterioration of cardiac electrophysiology and function [21].	Hypomethylated at 1.5 months after irradiation
	SLMAP also interacts with cardiac myosin suggesting a direct role in controlling cardiomyocyte contraction [22].	
LDLR (*Low Density Lipoprotein Receptor*)	Knockouts and/or mutations in *LDLR* lead to ineffective clearance of serum low density lipoprotein (LDL) cholesterol and contribute to premature atherosclerosis and cardiovascular disease [23].	Hypomethylated at 7 months after irradiation
ITPR2 (*Inositol 1,4,5-Trisphosphate Receptor Type 2*)	Certain polymorphs of *ITPR2* have been associated with higher systolic blood pressure. *ITPR2* is expressed widely in myocytes with altered expression in heart failure [24,25].	Hypomethylated at 7 months after irradiation
CDH18 (*Cadherin 18*)	A deletion involving *CDH18* was reported to be found in a case of congenital heart disease [26].	Hypomethylated at 1.5 months after irradiation
	In a study involving copy-number variants and the risk of sporadic congenital heart disease, rare deletions in study participants with congenital heart disease were in found in a number of genes including *CDH18* [27].	
CACNA1C (*Calcium Voltage-Gated Channel Subunit Alpha1 C*)	*CACNA1C* is a part of voltage-gated L-type calcium channel gene which plays an important role in cardiac electrical excitation [28].	Hypomethylated at 1.5 and 7 months after irradiation
CELF4 (*CUGBP Elav-like family member 4*)	A polymorphism of *CELF4* has been reported to have a modifying effect on anthracycline-related cardiomyopathy [29].	Hypomethylated at 7 months after irradiation
E2F6 (*E2F Transcription Factor 6*)	*E2F6* is a cell cycle regulator, abrogation of expression of *E2F6* in neonatal cardiac myocytes leads to a significant decrease in myocyte viability suggesting a role in myocardial regeneration [30,31].	Hypomethylated at 1.5 months after irradiation
	Forced *E2F6* expression activates gene expression in myocardium resulting in dilated cardiomyopathy [31].	
PTPN2 (*Protein Tyrosine Phosphatase Non-Receptor Type 2*)	Decreased expression of *PTPN2* through activation of miR-201 leads to attenuation of apoptosis and improvement of migration of cardiac stem cells exposed to hypoxia which would in turn increases their potential to repair the injured myocardium [32].	Hypomethylated at 7 months after irradiation

From STRING-db, multiple interactions were identified between dysregulated cardiac proteins and *LDLR* (calnexin), *ITPR2* (Phopholipase C beta3), *E2F* family (*RBBP7*) and *PTPN* family (*SLM2*, Thioredoxin, Ubiquiting-protein ligase B, galectin1, hrRNP K, cysteine and glycin-rich protein 1). In addition, two of the significantly dysregulated cardiac proteins were shown to interact with *CACNA1* family (Calsequestrin 2 and Myosin 4).

2.3. Hypomethylation of SLMAP at 1.5 Months Translates into a Dose-Dependent Increase in Gene Expression

Of the eight DMRs assessed by qPCR, only five genes were present in detectable quantities (*SLMAP*, *LDLR*, *ITPR2*, *E2F6* and *PTPN2*) (from now on called differentially methylated genes (DMGs)).

SLMAP expression was significantly increased after 1.5 months in all irradiated rats (Figure 4A). This increased expression follows the observed hypomethylation after 27.6 Gy FI (Table 1). Significantly increased *SLMAP* expression continues to 3 and 12 months after 0.92 Gy FI.

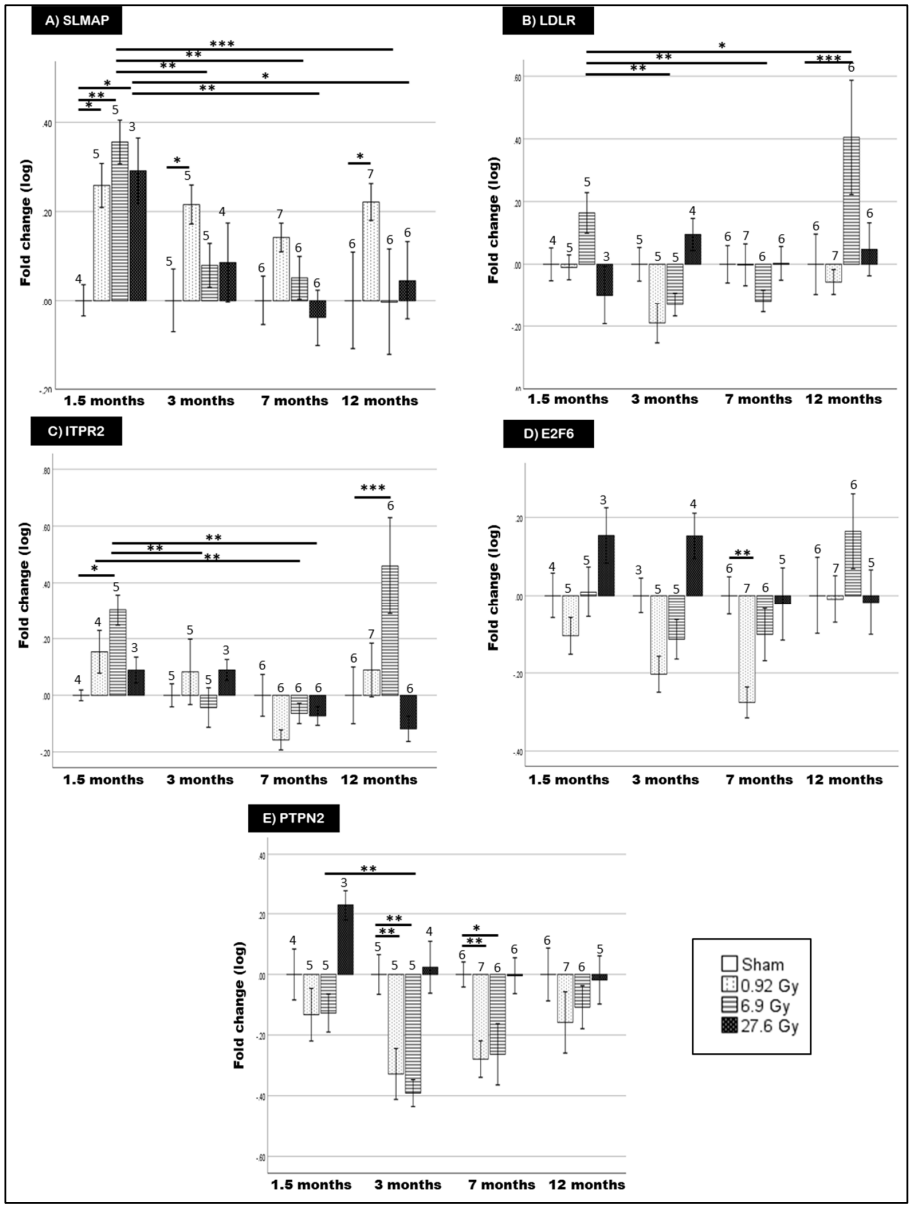

Figure 4. mRNA expression levels of *SLMAP* (**A**), *LDLR* (**B**), *ITPR2* (**C**), *E2F6* (**D**) and *PTPN2* (**E**) in the blood of rats receiving either sham irradiation (0 Gy) or fractionated irradiation of 0.92, 6.9 and 27.6 Gy and sampled after 1.5, 3, 7 and 12 months. Data are presented as log fold change normalized to *PHLPP1* (* = *p*-value < 0.05, ** < 0.01, *** < 0.001). Number of rats per group is indicated atop their respective bars. Plotted values represent group means ± standard error of mean (SEM). Statistical analysis was performed by SPSS General linear model and generalized linear models for data following normal and non-normal distribution, respectively. Multiple comparison correction was performed using Fisher's LSD.

For the other genes, *LDLR*, *ITPR2*, *E2F6* and *PTPN2* (Figure 4B–E), a number of gene expression alterations were detected, yet without consistent trends across radiation doses or follow-up time. Moreover, qPCR results did not reproduce the observed methylation pattern.

Correlation between DMG expression and rat GLS measurements identified a strong correlation between *E2F6* expression and the GLS of rats receiving 27.6 Gy FI ($r = |0.872|$, p-value < 0.05).

2.4. Two of the Selected Rat DMGs Show Altered Expression in BC Patient Blood

Patients of the MEDIRAD cohort with significantly higher cardiac radiation exposure showed a GLS-based subclinical left ventricular dysfunction (GLS decrease > 15%) 6 months after radiotherapy [33]. In the assayed BC patient blood, *SLMAP* showed a trend of increased expression for left-sided BC patients at V1 relative to V0, which decreases significantly at V2 (Figure 5A). Both *ITPR2* and *E2F6* showed increased expression at V1 relative to V0. However, the increase for *ITPR2* was only significant in right-sided BC patients, while for *E2F6* it was in left-sided BC patients (Figure 5C,D). On the other hand, LDLR and PTPN2 expression was unchanged (Figure 5B,E).

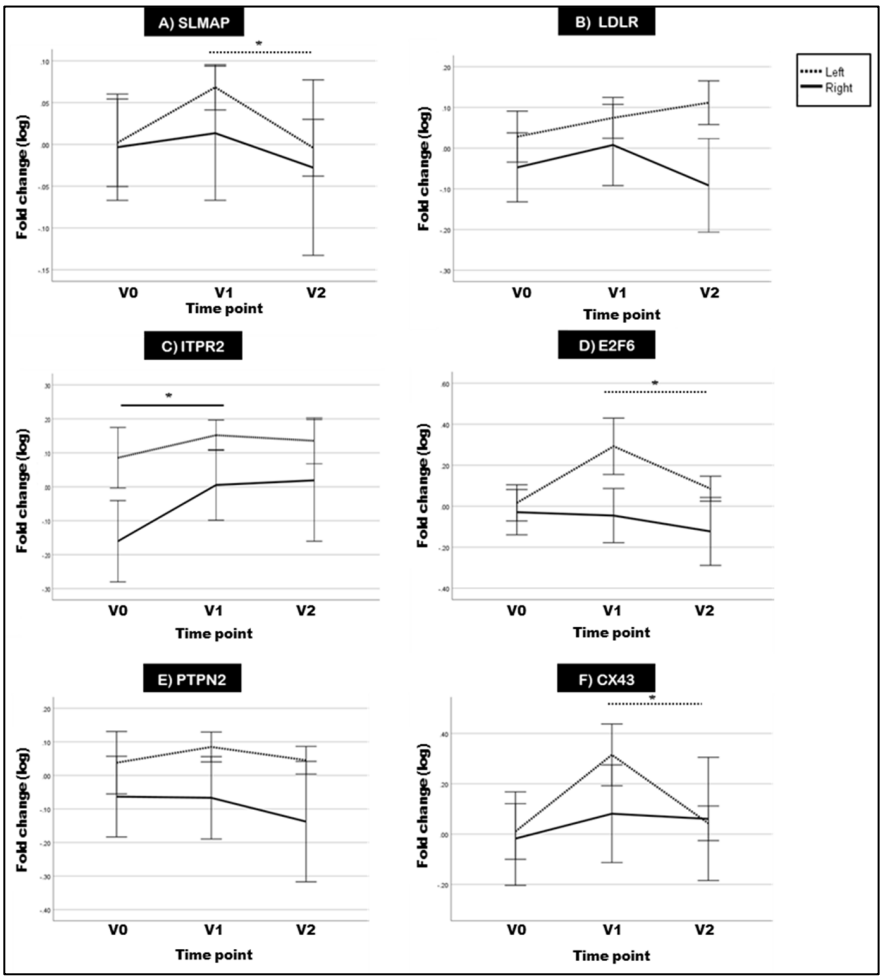

Figure 5. Mean log fold change of *SLMAP* (**A**), *LDLR* (**B**), *ITPR2* (**C**), *E2F6* (**D**), *PTPN* (**E**) and CX43 (*GJA1*) (**F**) expression in the blood of right- (n = 9) and left-sided (n = 16) BC patients sampled at diagnosis (V0), immediately after radiotherapy (V1) and 6 months after radiotherapy (V2). Data are presented as mean log fold changes in gene expression normalized to *TBP* ± SEM. Displayed significance values were calculated using observed log expression fold changes (* = p-value < 0.05). Statistical analysis was performed using SPSS generalized estimating equations module and multiple comparison correction was performed using LSD.

Previously, we demonstrated that selective inhibition of Connexin-43 (CX43) hemichannels alleviated radiation-induced endothelial cell damage [34]. In addition, *E2F6* was reported to affect the expression of CX43 gene (*GJA1*) in transgenic mice [31]. In our current experiments, we also found CX43 expression to be significantly increased at V1 in left-sided BC patient blood relative to V0 (Figure 5F).

In addition, patient stratification was performed according to whether the mean heart dose (MHD) was higher or lower than 2.5 Gy (Supplementary Figure S2). The 2.5 Gy MHD threshold was selected according to the German Society for Radiation Oncology (DEGRO) recommendations to minimize radiation-induced cardiotoxicity [35]. After stratification of data, the changes in *E2F6* and *SLMAP* were found to occur mainly at the higher radiation doses (>2.5 Gy). Correlation of MHD dose and gene expression indicated a medium correlation at V1 for *ITPR2*, *E2F6* and CX43 (*GJA1*) (*ITPR2*: r = |0.54|, *p*-value = 0.032; *E2F6*: r = |0.52|, *p*-value = 0.037; *GJA1*: r = |0.51|, *p*-value = 0.043) and at V2 for *SLMAP* (Pearson correlation coefficient r = |0.59|, *p*-value = 0.017).

3. Discussion

In the current study, we evaluated the effects of local heart irradiation on global and gene-specific DNA methylation in an experimental RICVD rat model. The validity of this model was previously confirmed by Ribeiro et al. who reported significant myocardial dysfunction (i.e., GLS decrease of >15%) at 12 and 18 months after 27.6 Gy FI [19]. Moreover, irradiated rats showed a decreased microvascular density (MVD) in apex of these rats' hearts which has been proposed as a predictor of early left ventricular remodeling [19]. Previous research investigating radiation-induced global methylation effects has reported variable effects of hyper- and hypo-methylation [36–38], as well as an occasional absence of methylation effects [39–41]. Our results showed global hypomethylation at 12 months for all doses while a hypomethylation trend was observed over time after 0.92 and 6.9 Gy FI. However, interpretation of our global methylation results is difficult due to the high inter-replicate variability and low sample numbers in certain groups. Nevertheless, a strong association between global methylation and GLS levels was observed at 12 months after the 2 higher doses (6.9 and 27.6 Gy). The global hypomethylation observed after 27.6 Gy follows previous reports linking global DNA methylation with cardiac dysfunction [42–45]. As for gene-specific methylation, higher numbers of hypomethylated DMRs were found at both 1.5 and 7 months after 27.6 Gy FI. Although there are limited studies addressing the effects of ionizing radiation on gene-specific methylation, most of these studies declare a higher predilection to hypermethylation [4,46]. However, the direction of gene specific methylation appears to vary according to employed animal model/cell line and irradiation protocol [4].

Pathway analysis of significant DMRs revealed dilated cardiomyopathy as an enriched pathway in rat blood at both 1.5 and 7 months. Interestingly, Ribeiro et al. (MEDIRAD colleagues) performed a proteomic analysis on the rats' cardiac tissues and also identified dilated cardiomyopathy as a significantly dysregulated protein pathway [19]. Other overlapping pathways between the rat DMRs (current study) and proteomics dataset [19] include cardiac muscle contraction, hypertrophic cardiomyopathy, adrenergic signaling in cardiomyocytes and longevity regulating pathway (DMRs at 1.5 months), as well as gonadotropin releasing hormone (GnRH) secretion, dopaminergic synapse, tight junction and circadian entrainment (DMRs at 7 months). All of these pathways have been previously implicated in cardiovascular impairment [47–56]. Dysregulation of these pathways has been known to result from oxidative stress, a proven contributor in radiation-induced cardiotoxicity [50,57–62]. Overall, pathway analyses of DMRs and proteomics datasets seem to support the occurrence of radiation-induced DNA methylation alterations in cardiac relevant genes which can affect functional protein levels.

Only *SLMAP* presented concurrent hypomethylation and overexpression at 1.5 months after 27.6 Gy FI. *SLMAP* represents a family of tail-anchored sarcolemmal membrane-associated proteins in the myocardium which regulates cardiac excitation-contraction [21,22,63]. Altered

SLMAP methylation was previously documented in advanced atherosclerotic plaques of coronary heart disease patients [64]. *SLMAP* can also inhibit Hippo signaling; a DMR enriched pathway at 1.5 months was previously associated with dilated cardiomyopathy and ischemic heart disease [65]. Specifically, Hippo pathway activation induces DNA damage-induced cardiomyocyte apoptosis after irradiation which is particularly relevant in the ensuing cardiac toxicity [66,67]. Consequently, the observed hypomethylation and overexpression may serve as a protective mechanism against radiation-induced cardiac effects by promoting cardiac regeneration and cardiomyocyte proliferation. However, as *SLMAP* overexpression gradually decreases at the later time points, these protective effects seem to be limited by time.

For the other DMGs (*LDLR*, *ITPR2*, *E2F6* and *PTPN2*), there was poor correlation between methylation status and gene expression. This discordance could be due to the occurrence of the DMRs primarily in gene body locations (c.f. gene promoters). While the exact function of gene body DNA methylation is poorly understood, hypothesized functions include inhibition of alternative splicing [68] and prevention of transcription initiation at intergenic promoters [69]. Previous research has indicated a positive correlation between gene body methylation and gene expression [70,71]. However, other studies have also shown a negative relationship between gene body methylation and gene expression [72–77]. This could be due to gene body CpGs representing functional elements such as enhancers, alternative promoters, transcription factor binding sites, repetitive elements and enrichment of nucleosomes at intron-exon junctions [70,74]. Therefore, these observations suggest that DNA methylation's regulation of gene expression is bidirectional with the location of CpG sites, disease context and relevant genes influencing the methylation effect [78].

Interestingly, Yao et al. previously reported the differential methylation of *E2F*, *PTPN* and *CDH* families in rat cardiac tissues after 6 months of acute 18 Gy of local heart irradiation [46]. As these rats also presented with RICVD, this suggests these gene families' responsiveness to radiation-induced methylation alterations. In addition, *CACNA1C*, a DMR exhibiting >25% differential methylation at 1.5 and 7 months, was also differentially methylated in RICVD rats after acute 18 Gy irradiation [46]. Despite not being detectable by qPCR in our samples, *CACNA1C* was identified in a number of our enriched DMR pathways concurrently dysregulated in the cardiac proteome including dilated cardiomyopathy and hypertrophic cardiomyopathy [19]. The reproducible enrichment of *CACNA1C* points to a role for *CACNA1C* in myocardial dysfunction with extrapolated relevance in RICVD [79,80]. Therefore, further investigations of *CACNA1C*'s methylation status after FI and its involvement in RICVD are warranted. From predicted STRING protein-protein interactions (PPI), significantly dysregulated cardiac proteins in the irradiated rats [19] were shown to interact with *LDLR*, *ITPR2*, *E2F, PTPN* and *CACNA1* families, as well as the methylation relevant *DNMT3a* [81,82]. This points to a multi-dimensional regulation of cardiac responses to ionizing radiation.

Finally, selected DMGs were explored in the blood of BC patients treated with adjuvant radiotherapy. *SLMAP* expression tended to increase at V1 compared to V0 in left-sided BC patients. Statistical significance was not reached, possibly due to the limited sample numbers and high inter-individual variation of DNA methylation, especially in blood [83–86]. Interestingly, after an initial increase at V1, *SLMAP* expression decreased at 6 months after radiotherapy (V2) in irradiated left-sided BC patients while presenting a medium correlation with MHD at V2. A similar initial *SLMAP* upregulation, which gradually decreases over time, was also observed in the irradiated rats. As decreased expression of *SLMAP* was found in human dilated ventricles, the observed *SLMAP* downregulation over time could contribute to cardiac dysfunction [22,87]. Interestingly, decreased *SLMAP* protein levels were also observed in cardiac tissues of Mayak workers diagnosed with ischemic heart diseases after occupational exposure to >500 mGy external gamma rays [88], which further supports the possible involvement of *SLMAP* in RICVD.

ITPR2 is the major cardiac isoform of a family of calcium channels whereby increased *ITPR2* expression activates calcium dependent signaling and modulates excitation-

contraction coupling in cardiomyocytes [25]. In addition, *ITPR2* overexpression has been linked to many cardiac pathologies including cardiac arrhythmias, failure and hypertrophy [25,89–91]. In our study, hypermethylation was associated with an increased expression of *ITPR2* for the 6.9 Gy FI dose at 1.5 and 12 months after irradiation in rats. In humans, right-sided BC patients showed significantly higher *ITPR2* expression at V1 relative to V0. Consequently, *ITPR2* dysregulation seems to occur as a result of radiation in both rats and BC patients.

E2F6 is a member of the *E2F* family that functions as a transcriptional repressor [92]. In-vivo, forced *E2F6* overexpression was associated with cardiac remodeling and dilated cardiomyopathy [31,93]. In addition, pathway analysis of Mayak nuclear workers' cardiac tissue proteomes showed that *E2F* family was dysregulated in irradiated groups compared to controls [94]. Our findings show *E2F6* hypomethylation at 1.5 months after 27.6 Gy FI in rats with variable expression and a seemingly dose-differential effect whereby low doses induce *E2F6* downregulation (c.f. 0.92 Gy), as shown in mouse embryos exposed to low-dose X-rays [95]. In addition, the strong correlation between *E2F6* and GLS alterations after 27.6 Gy FI suggests a possible contribution to the observed myocardial dysfunction. *E2F6* also exhibits significantly higher expression at V1 relative to V0 in left-sided patients. Stratification of patients, according to the received mean heart dose (MHD), showed *E2F6* dysregulation at higher MHDs (>2.5 Gy) in left-sided BC radiotherapy patients while maintaining a medium correlation to MHD. This further strengthens the potential involvement of *E2F6* in developing radiation-induced cardiac effects. However, further investigations in larger cohorts could help characterize the functional impact.

Finally, Connexin-43 (CX43) is a transmembrane protein forming gap junctions and hemichannels which are involved in intercellular communication [96]. CX43 was reported to increase the formation of atherosclerotic lesions in vivo [97,98]. We previously reported that single and fractionated X-irradiation induced an acute and persistent increase in CX43 gene and protein levels in human endothelial cells while selective inhibition of CX43 hemichannels alleviated radiation-induced endothelial cell damage [34,99]. In the current study, CX43 expression was significantly increased at V1 in the blood of left-sided BC patients relative to V0, in a similar manner to *E2F6*. Therefore, further investigation into the relationship between *E2F6* and CX43 in the scope of radiation-induced cardiovascular dysfunction is needed.

Study Limitations

Despite having the advantages of offering long-term longitudinal follow-up of identified DMRs over time, our study has a number of limitations. (1) Our first sampling time point for the rats was 1.5 months after irradiation. Consequently, we are unable to comment on any methylation alterations occurring at earlier time points. (2) Methylation analysis was performed in peripheral blood which introduces the confounder of different methylation profiles due to differing blood cell fraction counts [100–102]. DNA in blood is a mixture of DNA from blood cells and circulating cell-free DNA released from dying cells [102–104]. Local heart irradiation, as in our experimental rat irradiation model, primarily affects the methylation of the heart, as well as circulating blood cells. However, considering the short lifespan of circulating blood cells, delayed methylation alterations are most likely not the result of irradiated blood cells [105]. In addition, peripheral blood/leucocyte fraction methylation patterns have been frequently employed in DNA methylation biomarker research for cardiovascular disease identifying associations near genes unrelated to immune function or inflammation [106–108]. This supports the usefulness of blood-based DNA methylation investigations despite confounders, especially when considering the convenience of blood as a sample source. (3) The number of available samples was limited for certain rat sampling time points/doses due to technical limitations. (4) The primary validation in BC patients treated with adjuvant radiotherapy involved a somewhat limited number of patients (right-sided patients (n = 9) and left-sided patients (n = 16)) which necessitates confirmation in bigger patient cohorts.

4. Materials and Methods

4.1. Animals and Irradiation

Adult female Wistar rats (12–14 weeks old) underwent whole heart X-irradiation of 0.04, 0.3 and 1.2 Gy for 23 consecutive days (weekend excluded), resulting in cumulative doses of 0.92, 6.9 or 27.6 Gy. Control rats were sham-irradiated [0.0 Gy) following the same procedure. This translational experimental model was performed at MEDIRAD consortium partner, Centro Cardiovascular da Universidade de Lisboa (CCUL) [19]. There, blood was collected at 1.5, 3, 7 and 12 months after irradiation. Blood samples were received on dry ice and stored at −80 °C until further processing.

4.2. DNA Extraction

DNA was extracted from 200 µL frozen blood pellets using QIAamp DNA mini kit (Qiagen, Hilden, Germany) according to kit protocol. However, the extracted DNA concentration was found to be low [1–5 ng/µL). To increase the efficiency of DNA extraction, phenol/chloroform/isoamyl alcohol mixture [25:24:1 PCI) was incorporated into the DNA extraction protocol. Briefly, after sample thawing, samples were incubated with proteinase K and buffer AL at 56 °C for 10 min. 700 µL PCI was added per sample and mixed for 1.5 h at 1400 rpm at room temperature (Eppendorf Thermomixer C, Eppendorf AG, Hamburg, Germany). Next, samples were centrifuged for 5 min at 14,000× *g*. The upper aqueous layer containing the DNA was collected and 1–1.5 mL 100% ethanol as well as 50 µL buffer AL were added to precipitate the DNA. Finally, this mixture was transferred to QIAamp DNA mini kit column in 700 µL aliquots. Extraction was continued using QIAamp DNA mini kit following manufacturer recommendations. DNA concentration and purity were determined by comparing the ratio of optical density (OD) at 260 and 280 nm.

4.3. Global DNA Methylation Using MethylFlash Global DNA Methylation

Absolute global 5-methyl cytosine (5 mC) levels were analyzed in extracted DNA using MethylFlash Global DNA Methylation (5 mC) ELISA Easy Kit (Epigentek Group Inc., Farmingdale, NY, USA) according to manufacturer protocol. The kit measures 5 mC content as a percentage of total cytosine content. An amount of 100 ng of purified DNA was added to the ELISA plate. The methylated fraction of DNA was detected using 5 mC specific antibodies and quantified colorimetrically by measuring OD at 450 nm. The positive control (PC) supplied with the kit was used to generate a standard curve. The slope of the standard curve was calculated and used to determine the concentration of 5 mC in the samples as follows: 5 mC% = [(Sample OD − Negative control OD)/(Slope * DNA quantity)] × 100.

4.4. Gene-Specific DNA Methylation Analysis Using SureSelect Methyl-Seq

Gene-specific methylation analysis was performed with the Rat SureSelect Methyl-Seq platform (Agilent Technologies Inc., Santa Clara, CA, USA). SureSelect MethylSeq is a type of methylation capture sequencing (MC-seq) using biotinylated RNA baits to capture the genomic areas of interest for subsequent bisulfite sequencing. This method allows quantitative analysis of DNA methylation with single base resolution [109,110]. The rat SureSelect MethylSeq has been designed to target non-redundant promoters, CpG islands, island shores as well as previously identified GC-rich sequences [111]. Sixteen samples were selected to undergo SureSelect Methyl-Seq library preparation: sham-irradiated rats at 1.5 months (n = 4), 27.6 Gy irradiated rats at 1.5 months (n = 4), sham-irradiated rats at 7 months (n = 4) and 27.6 Gy irradiated rats at 7 months (n = 4). Due to technical limitations which necessitated high DNA sample concentrations [3 µg) with limited available blood per rat, sample size per group was limited. Library preparation and sequencing were performed in collaboration with the Ghent University sequencing facility NXTGNT (Ghent, Belgium) and GENEWIZ global genomics service company (GENEWIZ Germany GmbH, Leipzig, Germany). Library preparation, probe-based target enrichment, bisulfite treatment, and library indexing PCR were performed according to SureSelect^{XT} Methyl-Seq Library Preparation kit (Agilent Technologies Inc., Santa Clara, CA, USA) protocol (Version E0,

April 2018). The libraries were equimolarly pooled and sequenced together with a 20% PhiX control spike-in v3 on Illumina Hiseq 4000 (Illumina, Inc., San Diego, CA, USA), generating approximately 1.2×10^9 paired-end reads of 150 base pair length.

For the sequencing data analysis, similar methods were applied as was previously described [112]. Raw-read quality control was assessed using FASTQC (version 11.9). This was followed by reads trimming using Trim Galore (version 0.6.4) with the paired-end mode using the default parameters. Reads quality post trimming was reassessed as well (using FASTQC). Using bismark (version 0.19.0), reads were mapped to *Rattus norvegicus* genome which utilizes bowtie 2 (version 2.3.3), with a maximum of 1 mismatch in the seed region. The *Rattus norvegicus* reference genome (Rnor6.0) was downloaded from ftp://ftp.hgsc.bcm.edu/Rnorvegicus/Rnor6.0/, on 15 January 2020, and then indexed using Bismark with *bismark_genome_preparation* script. After mapping, these temporary changes were reverted. Subsequently, PCR duplications were removed using *deduplicate_bismark* script and a post-alignment quality control was performed using *flagstat* option of samtools (version 1.6) and *stats* option of BamUtil (version 1.0.14). The methylation level was assessed for each methylation context separately (for cytosines followed by guanines (CpGs), non-guanines and guanines (CHGs), two non-guanines (CHHs) or any other possibilities (CNs)). This was executed using *bismark_methylation_extractor* with the following flags: paired-end, no-overlap, and minimum coverage of at least 1 read, whilst the remaining parameters were set to the default settings.

For the rest of the analysis, only CpG methylations were included. For this, BSseq package (version 1.18.0) was used in Bioconductor. First, the data were smoothed using *BSmooth* function allowing 20 CpGs as a minimum within a window of 500, thereby smoothing the methylation levels across the CpGs within that window. This was used to establish thresholds for t-statistics (calculated using BSmooth.tstat function) across the groups using 1st and 99th quantile percentiles. Only CpGs with a minimum coverage of 10× within at least 3 samples were retained, and differentially methylation regions (DMRs) were identified using *dmrFinder* command. Each identified DMR was subjected to 1000 iterations of permutations (with randomization) that re-calculate the t-statistics for each permutation, and *p*-values were calculated and corrected using Benjamini-Hochberg false discovery rates (FDRs), for multiplicity problem. The *p*-values were calculated as the fraction of null areas (retrieved after each permutation) exceeding the observed area (before permutation). This was executed twice, performing pairwise comparison between sham-irradiated vs. 27.6 Gy at 1.5 and 7 months, separately. After that, DMRs were annotated to the rat genome (assembly Rnor_6.0) using closest from bedtools.

4.5. Pathway Analysis of Rat Differentially Methylated Regions (DMRs) by STRING-db

Pathway analysis of significant SureSelect MethylSeq DMRs (p-value < 0.05) at 1.5 and 7 months after 27.6 Gy or 0 Gy (sham) was performed using the STRING database (V.11.2). STRING is a database dedicated to organism-wide protein association networks by integrating known and predicted associations between proteins, including both physical interactions and functional associations [113]. The produced protein-protein interaction (PPI) network was then exported to Cytoscape 3.9.0 [114] where STRING enrichment was retrieved and enrichment maps were constructed using *EnrichmentMap* app in Cytoscape (V.3.3.3).

4.6. Investigation of Expression Alterations in DMRs Using Quantitative PCR

Validation of the rat DMRs was performed by quantitative Real Time PCR (qRT-PCR) in the blood of rats irradiated with 0, 0.92, 6.9 and 27.6 Gy FI at 1.5, 3, 7 and 12 months. Selection of the "top" target genes was performed by filtering the SureSelect MethylSeq output to show only DMRs with significant (p-value < 0.05) methylation difference (>25%) to limit downstream analyses [115–117]. Afterwards, a literature search of the filtered DMRs was performed to focus on genes with documented association to cardiovascular disease.

This led to 8 selected genes: *SLMAP*, *LDLR*, *ITPR2*, *CDH18*, *CACNA1C*, *CELF4*, *E2F6* and *PTPN2*. Only *SLMAP*, *LDLR*, *ITPR2*, *E2F6* and *PTPN2* were detectable in rat blood.

RNA was extracted from frozen rat blood using NucleoSpin RNA Blood Mini kit (Macherey-Nagel GmbH & Co. KG, Düren, Germany) according to manufacturer instructions. Then, reverse transcription of extracted RNA was performed using GoScript Reverse Transcription Mix employing random primers (Promega Corporation, Madison, WI, USA). Four genes were assayed as reference genes (*POLR2A*, *TBP*, *ACTB* and *PHLPP1*). Selection of the reference gene was performed using NormFinder [118] whereby *PHLPP1* showed the highest stability and was selected for normalization. The expression levels of selected DMR transcripts were determined by qPCR using TaqMan Gene Expression Assays (Thermo Fisher Scientific, Waltham, MA, USA) (*SLMAP*: Rn01401804_m1; *LDLR*: Rn00598442_m1; *ITPR2*: Rn00579067_m1; *E2F6*: Rn01499181_m1; *PTPN2*: Rn00588846_m1; *PHLPP1*: Rn00572211_m1). Next, qPCRs were performed using Fast Advanced Master Mix (Thermo Fisher Scientific, Waltham, MA, USA) on qTOWER^3 touch thermal cycler (Analytik Jena, Jena, Germany). Relative quantification was calculated using the equation $\log 2^{-\Delta\Delta CT}$, where $\Delta\Delta C_T = [C_T \text{ of target gene} - C_T \text{ of reference gene}]_{\text{irradiated group}} - [C_T \text{ of target gene} - C_T \text{ of reference gene}]_{\text{sham group}}$.

Significantly dysregulated proteins in cardiac tissues of rats receiving 27.6 Gy FI, supplied by MEDIRAD consortium partners [19], were queried in STRING-db (showing 50 interactors in 1st and 2nd shell) to reveal any relevant interactions with the rat DMGs.

4.7. Correlation of Rat Global DNA Methylation and DMR Expression with Global Longitudinal Strain (GLS)

MEDIRAD consortium partner, CCUL, evaluated the cardiac function of the irradiated rats and reported a dose-dependent reduction in GLS (>15%) [19]. 5 mC% levels and qPCR expression levels of rat DMGs were correlated with GLS in rats sacrificed at 12 months after irradiation.

4.8. Investigating Gene Expression of Selected DMRs in Breast Cancer Patients' Blood

4.8.1. Patient Selection

Blood pellets were collected from MEDIRAD EARLY HEART cohort of BC patients treated with adjuvant radiotherapy. This was performed at our consortium partner University Medical Center Groningen (UMCG), including a random selection of 25 BC patients with right-sided (n = 9) and left-sided BC (n = 16) [33]. The study was approved by the Ethics committee at UMCG (NL62360.042.17). Female unilateral BC patients aged 40–75 years treated with primary breast conserving surgery and postoperative radiotherapy were recruited during their first visit with the radiation oncologist. All patients signed a written informed consent form. Patients with previous medical history of coronary artery disease and/or myocardial infarction and/or atrial fibrillation were excluded. The patients were classified as having left- or right-sided BC according to the anatomical position of the tumor.

4.8.2. Radiotherapy Protocol

The total dose for the breast was 40.05–43.6 Gy. This dose was delivered in 15–20 separate fractions with a volumetric modulated arc therapy/fixed-field intensity-modulated radiotherapy (VMAT/IMRT) technique. Left-sided BC patients were treated with deep inspiration breath hold using the active breathing control system in order to lower the cardiac dose as much as possible.

4.8.3. Blood Collection and Reverse Transcription qPCR

Blood was collected from the patients in EDTA vacutainers at three time points: at diagnosis (V0), directly after radiotherapy (V1) and 6 months after radiotherapy (V2). Blood samples were centrifuged at 1500× *g* for 15 min to separate the plasma. Blood pellets were then stored at −80 °C until further processing. RNA extraction, cDNA synthesis and gene

expression analysis were performed using the same protocols detailed for the rat samples. TaqMan real-time PCR assays were used for qPCR quantification of *SLMAP*, *LDLR*, *ITPR2*, *E2F6*, *PTPN2* expression relative to reference gene, *TBP* (*SLMAP*: Hs01058330_g1; *LDLR*: Hs00181192_m1; *ITPR2*: Hs00181916_m1; *E2F6*: Hs01034552_m1; *PTPN2*: Hs00959888_g1; *TBP*: Hs00427620_m1).

4.9. Statistical Analysis

Normality of all datasets was assessed by Shapiro-Wilk test. Analysis of global methylation was performed using a generalized linear model with least significant difference (LSD) correction for multiple comparisons. Analysis of normally distributed parametric rat qPCR data was performed using a general linear model with LSD correction for multiple comparisons. For non-parametric rat qPCR data, analysis was performed using a generalized linear model with LSD correction for multiple comparisons. Correlation with functional data was performed by calculating Pearson correlation coefficient. Statistical analysis of BC patient qPCR data was performed using a generalized estimating equation to accommodate for the nonparametric characteristics of the data. All detailed statistical analyses were performed using SPSS version 28 (IBM Corp., Armonk, NY, USA).

5. Conclusions

The involvement of DNA methylation alterations in RICVD pathogenesis is underexplored. In the current study, we attempted to identify DNA methylation alterations related to rat whole-heart irradiation. The highest dose of radiation (27.6 Gy FI) resulted in blood DMRs associated with multiple cardiac relevant pathways including dilated cardiomyopathy and hypertrophic cardiomyopathy. This suggests the involvement of DNA methylation alterations in the onset of myocardial dysfunction. The expression of selected DMRs (significant differential methylation >25% with cardiovascular relevance) was assayed and discordance between methylation-predicted expression and observed expression suggests that gene body DNA methylation regulates gene expression in a multi-factorial bidirectional manner. *SLMAP*, *ITPR2*, *E2F6* and *PTPN2* showed differential methylation and expression in irradiated rats, while *E2F6* expression correlated with GLS measurements at 12 months after 27.6 Gy FI. Three of these rat DMGs (*SLMAP*, *ITPR2* and *E2F6*) also exhibited altered expression in BC patient blood, of which *SLMAP* and *E2F6* overexpression occurs mainly at higher MHDs. While this study provides some preliminary insights into radiation-induced DNA methylation alterations and their possible contribution to RICVD, further mechanistic validation by gene knockout/overexpression experiments, as well as large scale clinical studies are needed to validate their connections to RICVD.

Supplementary Materials: The following supporting information can be downloaded at: https://www.mdpi.com/article/10.3390/ijms232416214/s1.

Author Contributions: M.S. conducted all the experiments and wrote the manuscript text. M.M. performed the bioinformatics analyses. R.T. and S.C.R.S. performed the rat heart irradiation and blood sampling. S.C.R.S. provided the GLS functional data. A.P.G.C. and D.S. performed the breast cancer patients' blood sampling. F.V.N. and D.D. performed the SureSelect MethylSeq methylation analysis. S.B., P.-J.G., M.A.B., A.A. and R.R. contributed to designing the experiments and the supervision of the work. All authors contributed equally to reviewing the manuscript. All authors have read and agreed to the published version of the manuscript.

Funding: This project (MEDIRAD) has received funding from the Euratom research and training Horizon 2020, 2014–2018 programme under grant agreement No. 755523.

Institutional Review Board Statement: All animal procedures were performed according to Directive 2010/63/EU. The procedures were approved by the institutional Animal Welfare Body, licensed by DGAV, the Portuguese competent authority for animal protection (license number 0421/000/000/2018). For the human patients, the study protocol and related amendments received approval from Medisch Ethische Toetsingscommissie van het Universitair Medisch Centrum Groningen [METc UMCG], ID: METc 2017/379, NL62360.042.17.

Informed Consent Statement: Informed consent was obtained from all subjects involved in the study.

Data Availability Statement: The SureSelect methylation data presented in this study have been accessioned in the Sequence Read Archive (http://www.ncbi.nlm.nih.gov/sra) under BioProject Accession Number PRJNA808832.

Acknowledgments: We would like to thank the collaborators from our MEDIRAD partner institutes: Cardiovascular Center of the University of Lisbon (CCUL) and Universitair Medisch Centrum Groningen (UMCG). We also would like to thank Ana Rita S. Pereira, Filipe Rocha and Ana Teresa Pinto who are the team members at Centro Cardiovascular da Universidade de Lisboa (CCUL) that irradiated the animals during 23 consecutive days for the time points, sacrificed all animals as well as collected and prepared the blood samples. In addition, we would like to thank Richard Sang Un Lee from Johns Hopkins Medicine for his invaluable help and input. Finally, the authors are grateful to Irwin Cassells for critical reading of the manuscript.

Conflicts of Interest: The authors declare no conflict of interest.

References

1. Spetz, J.; Moslehi, J.; Sarosiek, K. Radiation-Induced Cardiovascular Toxicity: Mechanisms, Prevention, and Treatment. *Curr. Treat. Options Cardiovasc. Med.* **2018**, *20*, 31. [CrossRef] [PubMed]
2. Baselet, B.; Sonveaux, P.; Baatout, S.; Aerts, A. Pathological effects of ionizing radiation: Endothelial activation and dysfunction. *Cell. Mol. Life Sci.* **2019**, *76*, 699–728. [CrossRef] [PubMed]
3. Darby, S.C.; Ewertz, M.; McGale, P.; Bennet, A.M.; Blom-Goldman, U.; Brønnum, D.; Correa, C.; Cutter, D.; Gagliardi, G.; Gigante, B.; et al. Risk of Ischemic Heart Disease in Women after Radiotherapy for Breast Cancer. *N. Engl. J. Med.* **2013**, *368*, 987–998. [CrossRef] [PubMed]
4. Sallam, M.; Benotmane, M.A.; Baatout, S.; Guns, P.J.; Aerts, A. Radiation-induced cardiovascular disease: An overlooked role for DNA methylation? *Epigenetics* **2022**, *17*, 59–80. [CrossRef] [PubMed]
5. Jacob, S.; Pathak, A.; Franck, D.; Latorzeff, I.; Jimenez, G.; Fondard, O.; Lapeyre, M.; Colombier, D.; Bruguiere, E.; Lairez, O.; et al. Early detection and prediction of cardiotoxicity after radiation therapy for breast cancer: The BACCARAT prospective cohort study. *Radiat. Oncol.* **2016**, *11*. [CrossRef]
6. Walker, V.; Lairez, O.; Fondard, O.; Pathak, A.; Pinel, B.; Chevelle, C.; Franck, D.; Jimenez, G.; Camilleri, J.; Panh, L.; et al. Early detection of subclinical left ventricular dysfunction after breast cancer radiation therapy using speckle-tracking echocardiography: Association between cardiac exposure and longitudinal strain reduction (BACCARAT study). *Radiat. Oncol.* **2019**, *14*. [CrossRef]
7. Suelves, M.; Carrió, E.; Núñez-Álvarez, Y.; Peinado, M.A. DNA methylation dynamics in cellular commitment and differentiation. *Brief. Funct. Genom.* **2016**, *15*, 443–453. [CrossRef]
8. Schübeler, D. Function and information content of DNA methylation. *Nature* **2015**, *517*, 321–326. [CrossRef]
9. Wang, C.; Chen, L.; Yang, Y.; Zhang, M.; Wong, G. Identification of potential blood biomarkers for Parkinson's disease by gene expression and DNA methylation data integration analysis. *Clin. Epigenet.* **2019**, *11*, 24. [CrossRef]
10. Ahmed, S.A.H.; Ansari, S.A.; Mensah-Brown, E.P.K.; Emerald, B.S. The role of DNA methylation in the pathogenesis of type 2 diabetes mellitus. *Clin. Epigenet.* **2020**, *12*, 104. [CrossRef]
11. Locke, W.J.; Guanzon, D.; Ma, C.; Liew, Y.J.; Duesing, K.R.; Fung, K.Y.C.; Ross, J.P. DNA Methylation Cancer Biomarkers: Translation to the Clinic. *Front. Genet.* **2019**, *0*, 1150. [CrossRef] [PubMed]
12. Fernández-Sanlés, A.; Sayols-Baixeras, S.; Curcio, S.; Subirana, I.; Marrugat, J.; Elosua, R. DNA Methylation and Age-Independent Cardiovascular Risk, an Epigenome-Wide Approach. *Arterioscler. Thromb. Vasc. Biol.* **2018**, *38*, 645–652. [CrossRef] [PubMed]
13. Navas-Acien, A.; Domingo-Relloso, A.; Subedi, P.; Riffo-Campos, A.L.; Xia, R.; Gomez, L.; Haack, K.; Goldsmith, J.; Howard, B.V.; Best, L.G.; et al. Blood DNA Methylation and Incident Coronary Heart Disease: Evidence from the Strong Heart Study. *JAMA Cardiol.* **2021**, *6*, 1237. [CrossRef]
14. Lund, G.; Andersson, L.; Lauria, M.; Lindholm, M.; Fraga, M.F.; Villar-Garea, A.; Ballestar, E.; Esteller, M.; Zaina, S. DNA methylation polymorphisms precede any histological sign of atherosclerosis in mice lacking apolipoprotein E. *J. Biol. Chem.* **2004**, *279*, 29147–29154. [CrossRef] [PubMed]
15. Tabaei, S.; Tabaee, S.S. DNA methylation abnormalities in atherosclerosis. *Artif. Cells Nanomed. Biotechnol.* **2019**, *47*, 2031–2041. [CrossRef] [PubMed]
16. Jiang, D.; Sun, M.; You, L.; Lu, K.; Gao, L.; Hu, C.; Wu, S.; Chang, G.; Tao, H.; Zhang, D. DNA methylation and hydroxymethylation are associated with the degree of coronary atherosclerosis in elderly patients with coronary heart disease. *Life Sci.* **2019**, *224*, 241–248. [CrossRef]
17. Yamada, Y.; Horibe, H.; Oguri, M.; Sakuma, J.; Takeuchi, I.; Yasukochi, Y.; Kato, K.; Sawabe, M. Identification of novel hyper- or hypomethylated CpG sites and genes associated with atherosclerotic plaque using an epigenome-wide association study. *Int. J. Mol. Med.* **2018**, *41*, 2724–2732. [CrossRef]
18. Kumar, A.; Rai, P.S.; Upadhya, R.; Vishwanatha Shama Prasada, K.; Satish Rao, B.S.; Satyamoorthy, K. γ-radiation induces cellular sensitivity and aberrant methylation in human tumor cell lines. *Int. J. Radiat. Biol.* **2011**, *87*, 1086–1096. [CrossRef]

19. Ribeiro, S.; Simões, A.R.; Rocha, F.; Vala, I.S.; Pinto, A.T.; Ministro, A.; Poli, E.; Diegues, I.M.; Pina, F.; Benadjaoud, M.A.; et al. Molecular Changes in Cardiac Tissue as a New Marker to Predict Cardiac Dysfunction Induced By Radiotherapy. *Front. Oncol.* **2022**, *12*, 945521. [CrossRef]
20. Walker, V.; Crijns, A.; Langendijk, J.; Spoor, D.; Vliegenthart, R.; Combs, S.E.; Mayinger, M.; Eraso, A.; Guedea, F.; Fiuza, M.; et al. Early detection of cardiovascular changes after radiotherapy for Breast cancer: Protocol for a European multicenter prospective cohort study (MEDIRAD EARLY HEART study). *J. Med. Internet Res.* **2018**, *20*, e178. [CrossRef]
21. Nader, M.; Westendorp, B.; Hawari, O.; Salih, M.; Stewart, A.F.R.; Leenen, F.H.H.; Tuana, B.S. Tail-anchored membrane protein SLMAP is a novel regulator of cardiac function at the sarcoplasmic reticulum. *Am. J. Physiol. Heart Circ. Physiol.* **2012**, *302*. [CrossRef] [PubMed]
22. Nader, M. The SLMAP/Striatin complex: An emerging regulator of normal and abnormal cardiac excitation-contraction coupling. *Eur. J. Pharmacol.* **2019**, *858*, 172491. [CrossRef] [PubMed]
23. Franceschini, N.; Muallem, H.; Rose, K.M.; Boerwinkle, E.; Maeda, N. Low density lipoprotein receptor polymorphisms and the risk of coronary heart disease: The Atherosclerosis Risk in Communities Study. *J. Thromb. Haemost.* **2009**, *7*, 496–498. [CrossRef] [PubMed]
24. Wilker, E.; Mittleman, M.A.; Litonjua, A.A.; Poon, A.; Baccarelli, A.; Suh, H.; Wright, R.O.; Sparrow, D.; Vokonas, P.; Schwartz, J. Postural Changes in Blood Pressure Associated with Interactions between Candidate Genes for Chronic Respiratory Diseases and Exposure to Particulate Matter. *Environ. Health Perspect.* **2009**, *117*, 935–940. [CrossRef]
25. Sankar, N.; de Tombe, P.P.; Mignery, G.A. Calcineurin-NFATc Regulates Type 2 Inositol 1,4,5-Trisphosphate Receptor (InsP3R2) Expression during Cardiac Remodeling. *J. Biol. Chem.* **2014**, *289*, 6188. [CrossRef]
26. Chen, C.P.; Chang, S.Y.; Lin, C.J.; Chern, S.R.; Wu, P.S.; Chen, S.W.; Lai, S.T.; Chuang, T.Y.; Chen, W.L.; Yang, C.W.; et al. Prenatal diagnosis of a familial 5p14.3-p14.1 deletion encompassing CDH18, CDH12, PMCHL1, PRDM9 and CDH10 in a fetus with congenital heart disease on prenatal ultrasound. *Taiwan J. Obstet. Gynecol.* **2018**, *57*, 734–738. [CrossRef]
27. Soemedi, R.; Wilson, I.J.; Bentham, J.; Darlay, R.; Töpf, A.; Zelenika, D.; Cosgrove, C.; Setchfield, K.; Thornborough, C.; Granados-Riveron, J.; et al. Contribution of global rare copy-number variants to the risk of sporadic congenital heart disease. *Am. J. Hum. Genet.* **2012**, *91*, 489–501. [CrossRef]
28. Zhang, Q.; Chen, J.; Qin, Y.; Wang, J.; Zhou, L. Mutations in voltage-gated L-type calcium channel: Implications in cardiac arrhythmia. *Channels* **2018**, *12*, 201–218. [CrossRef]
29. Wang, X.; Sun, C.L.; Quiñones-Lombraña, A.; Singh, P.; Landier, W.; Hageman, L.; Mather, M.; Rotter, J.I.; Taylor, K.D.; Chen, Y.D.I.; et al. CELF4 variant and anthracycline-related cardiomyopathy: A children's oncology group genome-wide association study. *J. Clin. Oncol.* **2016**, *34*, 863–870. [CrossRef]
30. Movassagh, M.; Bicknell, K.A.; Brooks, G. Characterisation and regulation of E2F-6 and E2F-6b in the rat heart: A potential target for myocardial regeneration? *J. Pharm. Pharmacol.* **2006**, *58*, 73–82. [CrossRef]
31. Westendorp, B.; Major, J.L.; Nader, M.; Salih, M.; Leenen, F.H.H.; Tuana, B.S. The E2F6 repressor activates gene expression in myocardium resulting in dilated cardiomyopathy. *FASEB J.* **2012**, *26*, 2569–2579. [CrossRef] [PubMed]
32. Wang, B.; Gu, T.X.; Yu, F.M.; Zhang, G.W.; Zhao, Y. Overexpression of miR-210 promotes the potential of cardiac stem cells against hypoxia. *Scand. Cardiovasc. J.* **2018**, *52*, 367–371. [CrossRef] [PubMed]
33. Locquet, M.; Spoor, D.; Crijns, A.; van der Harst, P.; Eraso, A.; Guedea, F.; Fiuza, M.; Santos, S.C.R.; Combs, S.; Borm, K.; et al. Subclinical Left Ventricular Dysfunction Detected by Speckle-Tracking Echocardiography in Breast Cancer Patients Treated with Radiation Therapy: A Six-Month Follow-Up Analysis (MEDIRAD EARLY-HEART study). *Front. Oncol.* **2022**, *12*. [CrossRef]
34. Ramadan, R.; Vromans, E.; Anang, D.C.; Goetschalckx, I.; Hoorelbeke, D.; Decrock, E.; Baatout, S.; Leybaert, L.; Aerts, A. Connexin43 Hemichannel Targeting With TAT-Gap19 Alleviates Radiation-Induced Endothelial Cell Damage. *Front. Pharmacol.* **2020**, *11*, 212. [CrossRef] [PubMed]
35. Piroth, M.D.; Baumann, R.; Budach, W.; Dunst, J.; Feyer, P.; Fietkau, R.; Haase, W.; Harms, W.; Hehr, T.; Krug, D.; et al. Heart toxicity from breast cancer radiotherapy: Current findings, assessment, and prevention. *Strahlenther. Onkol.* **2019**, *195*, 1. [CrossRef] [PubMed]
36. Antwih, D.A.; Gabbara, K.M.; Lancaster, W.D.; Ruden, D.M.; Zielske, S.P. Radiation-induced epigenetic DNA methylation modification of radiation-response pathways. *Epigenetics* **2013**, *8*, 839–848. [CrossRef] [PubMed]
37. Koturbash, I.; Jadavji, N.M.; Kutanzi, K.; Rodriguez-Juarez, R.; Kogosov, D.; Metz, G.A.S.; Kovalchuk, O. Fractionated low-dose exposure to ionizing radiation leads to DNA damage, epigenetic dysregulation, and behavioral impairment. *Environ. Epigenet.* **2016**, *2*, dvw025. [CrossRef]
38. Loree, J.; Koturbash, I.; Kutanzi, K.; Baker, M.; Pogribny, I.; Kovalchuk, O. Radiation-induced molecular changes in rat mammary tissue: Possible implications for radiation-induced carcinogenesis. *Int. J. Radiat. Biol.* **2006**, *82*, 805–815. [CrossRef]
39. Jangiam, W.; Udomtanakunchai, C.; Reungpatthanaphong, P.; Tungjai, M.; Honikel, L.; Gordon, C.R.; Rithidech, K.N. Late Effects of Low-Dose Radiation on the Bone Marrow, Lung, and Testis Collected from the Same Exposed BALB/cJ Mice. *Dose Response* **2018**, *16*, 1503. [CrossRef]
40. Kuhmann, C.; Weichenhan, D.; Rehli, M.; Plass, C.; Schmezer, P.; Popanda, O. DNA methylation changes in cells regrowing after fractioned ionizing radiation. *Radiother. Oncol.* **2011**, *101*, 116–121. [CrossRef]
41. Maierhofer, A.; Flunkert, J.; Dittrich, M.; Müller, T.; Schindler, D.; Nanda, I.; Haaf, T. Analysis of global DNA methylation changes in primary human fibroblasts in the early phase following X-ray irradiation. *PLoS ONE* **2017**, *12*, e0177442. [CrossRef] [PubMed]

42. Li, J.; Zhang, M.; An, G.; Ma, Q. LncRNA TUG1 acts as a tumor suppressor in human glioma by promoting cell apoptosis. *Exp. Biol. Med.* **2016**, *241*, 644–649. [CrossRef]
43. Li, D.-X.; Fei, X.-R.; Dong, Y.-F.; Cheng, C.-D.; Yang, Y.; Deng, X.-F.; Huang, H.-L.; Niu, W.-X.; Zhou, C.-X.; Xia, C.-Y.; et al. The long non-coding RNA CRNDE acts as a ceRNA and promotes glioma malignancy by preventing miR-136-5p-mediated downregulation of Bcl-2 and Wnt2. *Oncotarget* **2017**, *8*, 88163–88178. [CrossRef] [PubMed]
44. Hu, C.-X. Relationship between global DNA methylation and hydroxymethylation levels in peripheral blood of elderly patients with myocardial infarction and the degree of coronary atherosclerosis. *J. Shanghai Jiaotong Univ. Med. Sci.* **2018**, *12*, 769–774.
45. Guarrera, S.; Fiorito, G.; Onland-Moret, N.C.; Russo, A.; Agnoli, C.; Allione, A.; Di Gaetano, C.; Mattiello, A.; Ricceri, F.; Chiodini, P.; et al. Gene-specific DNA methylation profiles and LINE-1 hypomethylation are associated with myocardial infarction risk. *Clin. Epigenet.* **2015**, *7*, 133. [CrossRef]
46. Yao, Y.; Chen, L.-F.; Li, J.; Chen, J.; Tian, X.-L.; Wang, H.; Mei, Z.-J.; Xie, C.-H.; Zhong, Y.-H. Altered DNA Methylation and Gene Expression Profiles in Radiation-Induced Heart Fibrosis of Sprague-Dawley Rats. *Radiat. Res.* **2022**. [CrossRef]
47. Yan, X.; Huang, Y.; Wu, J. Identify cross talk between circadian rhythm and coronary heart disease by multiple correlation analysis. *J. Comput. Biol.* **2018**, *25*, 1312–1327. [CrossRef] [PubMed]
48. Gibson, E.M.; Williams, I.I.I.W.P.; Kriegsfeld, L.J. Aging in the circadian system: Considerations for health, disease prevention and longevity. *Exp. Gerontol.* **2009**, *44*, 51–56. [CrossRef]
49. Cong, X.; Kong, W. Endothelial tight junctions and their regulatory signaling pathways in vascular homeostasis and disease. *Cell. Signal.* **2020**, *66*, 109485. [CrossRef]
50. Nikolaev, V.O.; Moshkov, A.; Lyon, A.R.; Miragoli, M.; Novak, P.; Paur, H.; Lohse, M.J.; Korchev, Y.E.; Harding, S.E.; Gorelik, J. β2-adrenergic receptor redistribution in heart failure changes cAMP compartmentation. *Science* **2010**, *327*, 1653–1657. [CrossRef]
51. Communal, C.; Colucci, W.S. The control of cardiomyocyte apoptosis via the beta-adrenergic signaling pathways. *Arch. Mal. Coeur Vaiss* **2005**, *98*, 236–241.
52. Sequeira, V.; Nijenkamp, L.L.A.M.; Regan, J.A.; van der Velden, J. The physiological role of cardiac cytoskeleton and its alterations in heart failure. *Biochim. Biophys. Acta (BBA) Biomembr.* **2014**, *1838*, 700–722. [CrossRef]
53. Packer, M. Longevity genes, cardiac ageing, and the pathogenesis of cardiomyopathy: Implications for understanding the effects of current and future treatments for heart failure. *Eur. Heart J.* **2020**, *41*, 3856–3861. [CrossRef]
54. Mokhles, M.M.; Trifirò, G.; Dieleman, J.P.; Haag, M.D.; van Soest, E.M.; Verhamme, K.M.C.; Mazzaglia, G.; Herings, R.; de Luise, C.; Ross, D.; et al. The risk of new onset heart failure associated with dopamine agonist use in Parkinson's disease. *Pharmacol. Res.* **2012**, *65*, 358–364. [CrossRef]
55. Yamaguchi, T.; Sumida, T.S.; Nomura, S.; Satoh, M.; Higo, T.; Ito, M.; Ko, T.; Fujita, K.; Sweet, M.E.; Sanbe, A.; et al. Cardiac dopamine D1 receptor triggers ventricular arrhythmia in chronic heart failure. *Nat. Commun.* **2020**, *11*, 4364. [CrossRef] [PubMed]
56. Azimzadeh, O.; Moertl, S.; Ramadan, R.; Baselet, B.; Laiakis, E.C.; Sebastian, S.; Beaton, D.; Hartikainen, J.M.; Kaiser, J.C.; Beheshti, A.; et al. Application of radiation omics in the development of adverse outcome pathway networks: An example of radiation-induced cardiovascular disease. *Int. J. Radiat. Biol.* **2022**, *98*, 1–30. [CrossRef] [PubMed]
57. Juárez Olguín, H.; Calderón Guzmán, D.; Hernández García, E.; Barragán Mejía, G. The role of dopamine and its dysfunction as a consequence of oxidative stress. *Oxid. Med. Cell Longev.* **2016**, *2016*, 9730467. [CrossRef] [PubMed]
58. Corbi, G.; Conti, V.; Russomanno, G.; Longobardi, G.; Furgi, G.; Filippelli, A.; Ferrara, N. Adrenergic signaling and oxidative stress: A role for sirtuins? *Front. Physiol.* **2013**, *4*, 324. [CrossRef]
59. Wilking, M.; Ndiaye, M.; Mukhtar, H.; Ahmad, N. Circadian rhythm connections to oxidative stress: Implications for human health. *Antioxid. Redox Signal.* **2013**, *19*, 192–208. [CrossRef]
60. Andersson, L.; Cinato, M.; Mardani, I.; Miljanovic, A.; Arif, M.; Koh, A.; Lindbom, M.; Laudette, M.; Bollano, E.; Omerovic, E.; et al. Glucosylceramide synthase deficiency in the heart compromises β1-adrenergic receptor trafficking. *Eur. Heart J.* **2021**, *42*, 4481–4492. [CrossRef]
61. Ramadan, R.; Baatout, S.; Aerts, A.; Leybaert, L. The role of connexin proteins and their channels in radiation-induced atherosclerosis. *Cell. Mol. Life Sci.* **2021**, *78*, 3087–3103. [CrossRef] [PubMed]
62. Gredilla, R.; Barja, G. Minireview: The Role of Oxidative Stress in Relation to Caloric Restriction and Longevity. *Endocrinology* **2005**, *146*, 3713–3717. [CrossRef] [PubMed]
63. Guzzo, R.M.; Salih, M.; Moore, E.D.; Tuana, B.S. Molecular properties of cardiac tail-anchored membrane protein SLMAP are consistent with structural role in arrangement of excitation-contraction coupling apparatus. *Am. J. Physiol. Heart Circ. Physiol.* **2005**, *288*, 1810–1819. [CrossRef] [PubMed]
64. Nazarenko, M.S.; Markov, A.V.; Lebedev, I.N.; Freidin, M.B.; Sleptcov, A.A.; Koroleva, I.A.; Frolov, A.V.; Popov, V.A.; Barbarash, O.L.; Puzyrev, V.P. A Comparison of Genome-Wide DNA Methylation Patterns between Different Vascular Tissues from Patients with Coronary Heart Disease. *PLoS ONE* **2015**, *10*, e0122601. [CrossRef] [PubMed]
65. Mia, M.M.; Singh, M.K. The Hippo Signaling Pathway in Cardiac Development and Diseases. *Front. Cell Dev. Biol.* **2019**, *7*. [CrossRef]
66. Yamamoto, S.; Yang, G.; Zablocki, D.; Liu, J.; Hong, C.; Kim, S.J.; Soler, S.; Odashima, M.; Thaisz, J.; Yehia, G.; et al. Activation of Mst1 causes dilated cardiomyopathy by stimulating apoptosis without compensatory ventricular myocyte hypertrophy. *J. Clin. Investig.* **2003**, *111*, 1463–1474. [CrossRef]
67. Bertini, E.; Oka, T.; Sudol, M.; Strano, S.; Blandino, G. At the crossroad between transformation and tumor suppression. *Cell Cycle* **2009**, *8*, 49–57. [CrossRef]

68. Jones, P.A. Functions of DNA methylation: Islands, start sites, gene bodies and beyond. *Nat. Rev. Genet.* **2012**, *13*, 484–492. [CrossRef]
69. Jjingo, D.; Conley, A.B.; Yi, S.V.; Lunyak, V.V.; Jordan, I.K. On the presence and role of human gene-body DNA methylation. *Oncotarget* **2012**, *3*, 462–474. [CrossRef]
70. Yang, X.; Han, H.; DeCarvalho, D.D.; Lay, F.D.; Jones, P.A.; Liang, G. Gene body methylation can alter gene expression and is a therapeutic target in cancer. *Cancer Cell* **2014**, *26*, 577–590. [CrossRef]
71. Spainhour, J.C.G.; Lim, H.S.; Yi, S.V.; Qiu, P. Correlation Patterns Between DNA Methylation and Gene Expression in The Cancer Genome Atlas. *Cancer Inform.* **2019**, *18*. [CrossRef] [PubMed]
72. Beltrami, C.M.; dos Reis, M.B.; Barros-Filho, M.C.; Marchi, F.A.; Kuasne, H.; Pinto, C.A.L.; Ambatipudi, S.; Herceg, Z.; Kowalski, L.P.; Rogatto, S.R. Integrated data analysis reveals potential drivers and pathways disrupted by DNA methylation in papillary thyroid carcinomas. *Clin. Epigenet.* **2017**, *9*, 45. [CrossRef] [PubMed]
73. Luan, Z.M.; Zhang, H.; Qu, X.L. Prediction efficiency of PITX2 DNA methylation for prostate cancer survival. *Genet. Mol. Res.* **2016**, *15*, 6750. [CrossRef] [PubMed]
74. Li, B.; Feng, Z.-H.; Sun, H.; Zhao, Z.-H.; Yang, S.-B.; Yang, P. The blood genome-wide DNA methylation analysis reveals novel epigenetic changes in human heart failure. *Eur. Rev. Med. Pharmacol. Sci.* **2017**, *21*, 1828–1836. [CrossRef] [PubMed]
75. Varley, K.E.; Gertz, J.; Bowling, K.M.; Parker, S.L.; Reddy, T.E.; Pauli-Behn, F.; Cross, M.K.; Williams, B.A.; Stamatoyannopoulos, J.A.; Crawford, G.E.; et al. Dynamic DNA methylation across diverse human cell lines and tissues. *Genome Res.* **2013**, *23*, 555–567. [CrossRef]
76. Kulis, M.; Heath, S.; Bibikova, M.; Queirós, A.C.; Navarro, A.; Clot, G.; Martínez-Trillos, A.; Castellano, G.; Brun-Heath, I.; Pinyol, M.; et al. Epigenomic analysis detects widespread gene-body DNA hypomethylation in chronic lymphocytic leukemia. *Nat. Genet.* **2012**, *44*, 1236–1242. [CrossRef]
77. Maunakea, A.K.; Nagarajan, R.P.; Bilenky, M.; Ballinger, T.J.; Dsouza, C.; Fouse, S.D.; Johnson, B.E.; Hong, C.; Nielsen, C.; Zhao, Y.; et al. Conserved role of intragenic DNA methylation in regulating alternative promoters. *Nature* **2010**, *466*, 253–257. [CrossRef]
78. Yang, Q.; Wu, F.; Wang, F.; Cai, K.; Zhang, Y.; Sun, Q.; Zhao, X.; Gui, Y.; Li, Q. Impact of DNA methyltransferase inhibitor 5-azacytidine on cardiac development of zebrafish in vivo and cardiomyocyte proliferation, apoptosis, and the homeostasis of gene expression in vitro. *J. Cell. Biochem.* **2019**, *120*, 17459–17471. [CrossRef]
79. Chu, Q.; Li, A.; Chen, X.; Qin, Y.; Sun, X.; Li, Y.; Yue, E.; Wang, C.; Ding, X.; Yan, Y.; et al. Overexpression of miR-135b attenuates pathological cardiac hypertrophy by targeting CACNA1C. *Int. J. Cardiol.* **2018**, *269*, 235–241. [CrossRef]
80. Li, Z.; Wang, X.; Wang, W.; Du, J.; Wei, J.; Zhang, Y.; Wang, J.; Hou, Y. Altered long non-coding RNA expression profile in rabbit atria with atrial fibrillation: TCONS_00075467 modulates atrial electrical remodeling by sponging miR-328 to regulate CACNA1C. *J. Mol. Cell. Cardiol.* **2017**, *108*, 73–85. [CrossRef]
81. Deplus, R.; Blanchon, L.; Rajavelu, A.; Boukaba, A.; Defrance, M.; Luciani, J.; Rothé, F.; Dedeurwaerder, S.; Denis, H.; Brinkman, A.B.; et al. Regulation of DNA Methylation Patterns by CK2-Mediated Phosphorylation of Dnmt3a. *Cell Rep.* **2014**, *8*, 743–753. [CrossRef] [PubMed]
82. Weinberg, D.N.; Rosenbaum, P.; Chen, X.; Barrows, D.; Horth, C.; Marunde, M.R.; Popova, I.K.; Gillespie, Z.B.; Keogh, M.-C.; Lu, C.; et al. Two competing mechanisms of DNMT3A recruitment regulate the dynamics of de novo DNA methylation at PRC1-targeted CpG islands. *Nat. Genet.* **2021**, *53*, 794–800. [CrossRef] [PubMed]
83. Chatterjee, A.; Stockwell, P.A.; Rodger, E.J.; Duncan, E.J.; Parry, M.F.; Weeks, R.J.; Morison, I.M. Genome-wide DNA methylation map of human neutrophils reveals widespread inter-individual epigenetic variation. *Sci. Rep.* **2015**, *5*, 17328. [CrossRef] [PubMed]
84. Davies, M.N.; Volta, M.; Pidsley, R.; Lunnon, K.; Dixit, A.; Lovestone, S.; Coarfa, C.; Harris, R.A.; Milosavljevic, A.; Troakes, C.; et al. Functional annotation of the human brain methylome identifies tissue-specific epigenetic variation across brain and blood. *Genome Biol.* **2012**, *13*, R43. [CrossRef]
85. de la Rocha, C.; Zaina, S.; Lund, G. Is Any Cardiovascular Disease-Specific DNA Methylation Biomarker within Reach? *Curr. Atheroscler. Rep.* **2020**, *22*, 62. [CrossRef]
86. Veenstra, C.; Karlsson, E.; Mirwani, S.M.; Nordenskjöld, B.; Fornander, T.; Pérez-Tenorio, G.; Stål, O. The effects of PTPN2 loss on cell signalling and clinical outcome in relation to breast cancer subtype. *J. Cancer Res. Clin. Oncol.* **2019**, *145*, 1845–1856. [CrossRef]
87. Nader, M.; Alsolme, E.; Alotaibi, S.; Alsomali, R.; Bakheet, D.; Dzimiri, N. SLMAP-3 is downregulated in human dilated ventricles and its overexpression promotes cardiomyocyte response to adrenergic stimuli by increasing intracellular calcium. *Can. J. Physiol. Pharmacol.* **2019**, *97*, 623–630. [CrossRef]
88. Azimzadeh, O.; Azizova, T.; Merl-Pham, J.; Blutke, A.; Moseeva, M.; Zubkova, O.; Anastasov, N.; Feuchtinger, A.; Hauck, S.M.; Atkinson, M.J. Chronic occupational exposure to ionizing radiation induces alterations in the structure and metabolism of the heart: A proteomic analysis of human formalin-fixed paraffin-embedded (FFPE) cardiac tissue. *Int. J. Mol. Sci.* **2020**, *21*, 6832. [CrossRef]
89. Natesan, S.; Maxwell, J.T.; Hale, P.R.; Mignery, G.A. Abstract 298: CaMKII-Mediated Phosphorylation of InsP3R2 Activates Hypertrophic Gene Transcription. *Circ. Res.* **2012**, *111*, A298. [CrossRef]
90. Harzheim, D.; Talasila, A.; Movassagh, M.; Foo, R.S.-Y.; Figg, N.; Bootman, M.D.; Roderick, H.L. Elevated InsP3R expression underlies enhanced calcium fluxes and spontaneous extra-systolic calcium release events in hypertrophic cardiac myocytes. *Channels* **2010**, *4*, 67–71. [CrossRef]
91. Santulli, G.; Chen, B.; Forrester, F.; Wu, H.; Reiken, S.; Marks, A.R. Abstract 16984: Role of Inositol 1,4,5-Triphosphate Receptor 2 in Post-Ischemic Heart Failure. *Circulation* **2014**, *130*, A16984. [CrossRef]

92. Oberley, M.J.; Inman, D.R.; Farnham, P.J. E2F6 negatively regulates BRCA1 in human cancer cells without methylation of histone H3 on lysine 9. *J. Biol. Chem.* **2003**, *278*, 42466–42476. [CrossRef] [PubMed]
93. Major, J.L.; Dewan, A.; Salih, M.; Leddy, J.J.; Tuana, B.S. E2F6 Impairs Glycolysis and Activates BDH1 Expression Prior to Dilated Cardiomyopathy. *PLoS ONE* **2017**, *12*, e0170066. [CrossRef] [PubMed]
94. Azimzadeh, O.; Azizova, T.; Merl-Pham, J.; Subramanian, V.; Bakshi, M.V.; Moseeva, M.; Zubkova, O.; Hauck, S.M.; Anastasov, N.; Atkinson, M.J.; et al. A dose-dependent perturbation in cardiac energy metabolism is linked to radiation-induced ischemic heart disease in Mayak nuclear workers. *Oncotarget* **2017**, *8*, 9067–9078. [CrossRef] [PubMed]
95. Verheyde, J.; de Saint-Georges, L.; Leyns, L.; Benotmane, M.A. The Role of Trp53 in the Transcriptional Response to Ionizing Radiation in the Developing Brain. *DNA Res.* **2006**, *13*, 65–75. [CrossRef]
96. Sáez, J.C.; Retamal, M.A.; Basilio, D.; Bukauskas, F.F.; Bennett, M.V.L. Connexin-based gap junction hemichannels: Gating mechanisms. *Biochim. Biophys. Acta* **2005**, *1711*, 215. [CrossRef]
97. Wong, C.W.; Burger, F.; Pelli, G.; Mach, F.; Kwak, B.R. Dual benefit of reduced Cx43 on atherosclerosis in LDL receptor-deficient mice. *Cell Commun. Adhes.* **2003**, *10*, 395–400. [CrossRef]
98. Kwak, B.R.; Veillard, N.; Pelli, G.; Mulhaupt, F.; James, R.W.; Chanson, M.; Mach, F. Reduced connexin43 expression inhibits atherosclerotic lesion formation in low-density lipoprotein receptor-deficient mice. *Circulation* **2003**, *107*, 1033–1039. [CrossRef]
99. Ramadan, R.; Vromans, E.; Anang, D.C.; Decrock, E.; Mysara, M.; Monsieurs, P.; Baatout, S.; Leybaert, L.; Aerts, A. Single and fractionated ionizing radiation induce alterations in endothelial connexin expression and channel function. *Sci. Rep.* **2019**, *9*. [CrossRef]
100. Sharma, P.; Sahni, N.S.; Tibshirani, R.; Skaane, P.; Urdal, P.; Berghagen, H.; Jensen, M.; Kristiansen, L.; Moen, C.; Sharma, P.; et al. Early detection of breast cancer based on gene-expression patterns in peripheral blood cells. *Breast. Cancer Res.* **2005**, *7*, R634. [CrossRef]
101. Wu, H.C.; Delgado-Cruzata, L.; Flom, J.D.; Kappil, M.; Ferris, J.S.; Liao, Y.; Santella, R.M.; Terry, M.B. Global methylation profiles in DNA from different blood cell types. *Epigenetics* **2011**, *6*, 76. [CrossRef] [PubMed]
102. Li, L.; Choi, J.Y.; Lee, K.M.; Sung, H.; Park, S.K.; Oze, I.; Pan, K.F.; You, W.C.; Chen, Y.X.; Fang, J.Y.; et al. DNA Methylation in Peripheral Blood: A Potential Biomarker for Cancer Molecular Epidemiology. *J. Epidemiol.* **2012**, *22*, 384. [CrossRef] [PubMed]
103. Zemmour, H.; Planer, D.; Magenheim, J.; Moss, J.; Neiman, D.; Gilon, D.; Korach, A.; Glaser, B.; Shemer, R.; Landesberg, G.; et al. Non-invasive detection of human cardiomyocyte death using methylation patterns of circulating DNA. *Nat. Commun.* **2018**, *9*, 1443. [CrossRef] [PubMed]
104. Liu, Q.; Ma, J.; Deng, H.; Huang, S.J.; Rao, J.; Xu WBin Huang, J.S.; Sun, S.Q.; Zhang, L. Cardiac-specific methylation patterns of circulating DNA for identification of cardiomyocyte death. *BMC Cardiovasc. Disord.* **2020**, *20*, 310. [CrossRef] [PubMed]
105. Scheiermann, C.; Frenette, P.S.; Hidalgo, A. Regulation of leucocyte homeostasis in the circulation. *Cardiovasc. Res.* **2015**, *107*, 340. [CrossRef]
106. Ma, S.C.; Zhang, H.P.; Kong, F.Q.; Zheng, H.; Yang, C.; He, Y.Y.; Wang, Y.H.; Yang, A.N.; Tian, J.; Yang, X.L.; et al. Integration of gene expression and DNA methylation profiles provides a molecular subtype for risk assessment in atherosclerosis. *Mol. Med. Rep.* **2016**, *13*, 4791–4799. [CrossRef]
107. Agha, G.; Mendelson, M.M.; Ward-Caviness, C.K.; Joehanes, R.; Huan, T.X.; Gondalia, R.; Salfati, E.; Brody, J.A.; Fiorito, G.; Bressler, J.; et al. Blood Leukocyte DNA Methylation Predicts Risk of Future Myocardial Infarction and Coronary Heart Disease. *Circulation* **2019**, *140*, 645–657. [CrossRef]
108. Huan, T.; Joehanes, R.; Song, C.; Peng, F.; Guo, Y.; Mendelson, M.; Yao, C.; Liu, C.; Ma, J.; Richard, M.; et al. Genome-wide identification of DNA methylation QTLs in whole blood highlights pathways for cardiovascular disease. *Nat. Commun.* **2019**, *10*, 4267. [CrossRef]
109. Lee, J.R.; Ryu, D.S.; Park, S.J.; Choe, S.H.; Cho, H.M.; Lee, S.R.; Kim, S.U.; Kim, Y.H.; Huh, J.W. Successful application of human-based methyl capture sequencing for methylome analysis in non-human primate models. *BMC Genom.* **2018**, *19*, 267. [CrossRef]
110. Shu, C.; Zhang, X.; Aouizerat, B.E.; Xu, K. Comparison of methylation capture sequencing and Infinium MethylationEPIC array in peripheral blood mononuclear cells. *Epigenet. Chromatin* **2020**, *13*, 1–15. [CrossRef]
111. Carey, J.L.; Cox, O.H.; Seifuddin, F.; Marque, L.; Tamashiro, K.L.; Zandi, P.P.; Wand, G.S.; Lee, R.S. A Rat Methyl-Seq Platform to Identify Epigenetic Changes Associated with Stress Exposure. *J. Vis. Exp.* **2018**, *140*, 58617. [CrossRef] [PubMed]
112. Seifuddin, F.; Wand, G.; Cox, O.; Pirooznia, M.; Moody, L.; Yang, X.; Tai, J.; Boersma, G.; Tamashiro, K.; Zandi, P.; et al. Genome-wide Methyl-Seq analysis of blood-brain targets of glucocorticoid exposure. *Epigenetics* **2017**, *12*, 637–652. [CrossRef] [PubMed]
113. Szklarczyk, D.; Gable, A.L.; Nastou, K.C.; Lyon, D.; Kirsch, R.; Pyysalo, S.; Doncheva, N.T.; Legeay, M.; Fang, T.; Jensen, L.J.; et al. The STRING database in 2021: Customizable protein-protein networks, and functional characterization of user-uploaded gene/measurement sets. *Nucleic Acids Res.* **2021**, *49*, 605–612. [CrossRef]
114. Shannon, P.; Markiel, A.; Ozier, O.; Baliga, N.S.; Wang, J.T.; Ramage, D.; Amin, N.; Schwikowski, B.; Ideker, T. Cytoscape: A Software Environment for Integrated Models of Biomolecular Interaction Networks. *Genome Res.* **2003**, *13*, 2498. [CrossRef] [PubMed]

115. Reinert, T.; Modin, C.; Castano, F.M.; Lamy, P.; Wojdacz, T.K.; Hansen, L.L.; Wiuf, C.; Borre, M.; Dyrskjøt, L.; Ørntoft, T.F. Comprehensive genome methylation analysis in bladder cancer: Identification and validation of novel methylated genes and application of these as urinary tumor markers. *Clin. Cancer Res.* **2011**, *17*, 5582–5592. [CrossRef]
116. Chernoff, M.B.; Demanelis, K.; Gillard, M.; Delgado, D.; Griend DJVander Pierce, B.L. Abstract 160: Identifying differential methylation patterns of benign and tumor prostate tissue in African American and European American prostate cancer patients. *Cancer Res.* **2020**, *80*, 160. [CrossRef]
117. Tarr, I.S.; McCann, E.P.; Benyamin, B.; Peters, T.J.; Twine, N.A.; Zhang, K.Y.; Zhao, Q.; Zhang, Z.H.; Rowe, D.B.; Nicholson, G.A.; et al. Monozygotic twins and triplets discordant for amyotrophic lateral sclerosis display differential methylation and gene expression. *Sci. Rep.* **2019**, *9*, 8254. [CrossRef]
118. Andersen, C.L.; Jensen, J.L.; Ørntoft, T.F. Normalization of real-time quantitative reverse transcription-PCR data: A model-based variance estimation approach to identify genes suited for normalization, applied to bladder and colon cancer data sets. *Cancer Res.* **2004**, *64*, 5245–5250. [CrossRef]